Published in final edited form as:

Converg Sci Phys Oncol. 2017 ; 3: . doi:10.1088/2057-1739/aa9263.

Matrix Stiffness Enhances VEGFR-2 Internalization, Signaling, and Proliferation in Endothelial Cells

Danielle J. LaValley[1], **Matthew R. Zanotelli**[1], **Francois Bordeleau**[2], **Wenjun Wang**[2], **Samantha C. Schwager**[2], and **Cynthia A. Reinhart-King**[1,2,*]

[1]Nancy E. and Peter C. Meinig School of Biomedical Engineering, Cornell University, Ithaca, NY 14853

[2]Department of Biomedical Engineering, Vanderbilt University, Nashville, TN 37235

Abstract

Vascular endothelial growth factor (VEGF) can mediate endothelial cell migration, proliferation, and angiogenesis. During cancer progression, VEGF production is often increased to stimulate the growth of new blood vessels to supply growing tumors with the additional oxygen and nutrients they require. Extracellular matrix stiffening also occurs during tumor progression, however, the crosstalk between tumor mechanics and VEGF signaling remains poorly understood. Here, we show that matrix stiffness heightens downstream endothelial cell response to VEGF by altering VEGF receptor-2 (VEGFR-2) internalization, and this effect is influenced by cell confluency. In sub-confluent endothelial monolayers, VEGFR-2 levels, but not VEGFR-2 phosphorylation, are influenced by matrix rigidity. Interestingly, more compliant matrices correlated with increased expression and clustering of VEGFR-2; however, stiffer matrices induced increased VEGFR-2 internalization. These effects are most likely due to actin-mediated contractility, as inhibiting ROCK on stiff substrates increased VEGFR-2 clustering and decreased internalization. Additionally, increasing matrix stiffness elevates ERK 1/2 phosphorylation, resulting in increased cell proliferation. Moreover, cells on stiff matrices generate more actin stress fibers than on compliant substrates, and the addition of VEGF stimulates an increase in fiber formation regardless of stiffness. In contrast, once endothelial cells reached confluency, stiffness-enhanced VEGF signaling was no longer observed. Together, these data show a complex effect of VEGF and matrix mechanics on VEGF-induced signaling, receptor dynamics, and cell proliferation that is mediated by cell confluency.

Keywords

Endothelial cells; extracellular matrix; matrix stiffness; VEGF; proliferation

Introduction

Angiogenesis, the formation of new blood vessels from pre-existing vessels, is regulated by a balance between pro- and anti-angiogenic cues. During various diseases, including cancer,

*To whom correspondence should be addressed: Cynthia A. Reinhart-King, Department of Biomedical Engineering, Vanderbilt University, PMB 351631, Nashville, TN 37235, Phone: 615-875-8309, cynthia.reinhart-king@vanderbilt.edu.

angiogenesis can become dysregulated [1]. The blood vessels that form around tumors are hyperpermeable, immature, and organized in tortuous patterns [1,2]. The resulting abnormal vascular geometries promote chaotic blood flow and high interstitial fluid pressure gradients, as well as contribute to a hypoxic, acidic tumor core [3]. Together, these features contribute to inefficient delivery of chemotherapeutics to the tumor. As such, an emerging cancer treatment strategy seeks to “normalize” the tumor-associated vasculature by restoring the imbalance between pro- and anti-angiogenic cues to increase the delivery and efficacy of therapeutics [4].

Elevated levels of pro-angiogenic vascular endothelial growth factor (VEGF) are often reported in cancer patients, correlating with the degree of malignancy [5]. VEGF is considered to be a major contributing factor in promoting aberrant tumor vasculature [1,6]. Angiogenesis is predominately mediated through the interaction of VEGF-A with VEGF receptor-2 (VEGFR-2) [7]. Activation of VEGFR-2, through ligand binding or mechanical stimuli such as shear stress, requires receptor dimerization and trans-autophosphorylation on intracellular tyrosine residues [8]. Downstream signals such as focal adhesion kinase (FAK), extracellular signal-regulated kinase (ERK) 1/2, protein kinase B (PKB/Akt), and endothelial nitric oxide synthase (eNOS) are then activated and mediate endothelial cell behaviors including migration, proliferation, survival, and permeability [9].

In addition to the abnormal growth of blood vessels in the tumor microenvironment, many other microenvironmental changes are known to occur during tumor progression that can influence tumor growth. One such change is an increase in extracellular matrix (ECM) stiffness within the tumor due to increased ECM protein production and increased crosslinking of existing matrix proteins within the tumor stroma [10,11]. Altered matrix mechanics is known to influence cell behaviors [12,13] mainly through crosstalk between integrins and the Rho/ROCK pathway [14]. More specifically, matrix stiffness has been shown to affect endothelial gene expression [15,16], morphology [17–20], outgrowth [21], traction forces [22–24], and permeability [24–27].

Cellular behavior is determined by the complex integration of numerous chemical and mechanical cues [28,29]. While some have begun to delineate the pathways of these chemical and mechanical cues and identify crosstalk mechanisms [30–37], most are not yet fully understood. Here, the combined effects of matrix rigidity and VEGF stimulation on endothelial cell behavior were investigated. Our data indicate that ECM stiffness increases endothelial cell VEGFR-2 internalization and downstream VEGF-stimulated signaling, proliferation, and stress fiber formation.

Materials and Methods

Cell Culture

Human umbilical vein endothelial cells (HUVECs) were purchased from Lonza (Walkersville, MD). They were maintained and plated at 37°C and 5% CO_2 in endothelial growth medium (EGM; Lonza) supplemented with the EGM BulletKit^{TM} (2% v/v FBS, Bovine Brain Extract, Ascorbic Acid, Hydrocortisone, Epidermal Growth Factor, Gentamicin/Amphotericin-B; Lonza). HUVECs were used at passage 4 for all experiments.

Polyacrylamide Gel Fabrication

Polyacrylamide (PA) gels were fabricated as described elsewhere [18,22,38]. Briefly, the ratio of acrylamide (40% w/v; Bio-Rad, Hercules, CA) and bis-acrylamide (2% w/v; Bio-Rad) was varied to tune gel stiffness from 1 to 10 kPa to mimic vascular and tumorous tissue as described previously [22,26,39]. Gels were coated with either 0.1 mg/ml collagen type I (BD Biosciences, San Jose, CA) or fibronectin (Thermo Fisher Scientific, Waltham, MA).

Western Blot

The seeding density of HUVECs atop PA gels or collagen-coated glass coverslips was optimized to achieve either 50–70% confluency after one day or full confluence after 2–4 days. Cells were stimulated with 5 ng/ml human recombinant $VEGF_{165}$ (R&D Systems, Minneapolis, MN) for the desired time, rinsed with ice cold phosphate buffered saline (PBS), and lysed with 6x SDS sample buffer (4x Tris-Cl/SDS, pH 6.8, 30% v/v glycerol, 10% w/v SDS, 0.09% v/v 2-mecaptoethanol, and 0.012% w/v Bromophenol Blue) [40]. For Western blotting, lysates were run with 8% w/v acrylamide gels on a Mini-PROTEAN Tetra System (Bio-Rad) and electrotransferred onto a PVDF membrane (Bio-Rad). Membranes were blocked in 5% w/v BSA (Sigma-Aldrich, St. Louis, MO) or milk (Nestle) in 0.1% v/v Tris-buffered saline (TBS)-polyoxyethylene 20 sorbitan monolaurate (Tween; JT Baker, Phillipsburg, NJ) for 1 h. Membranes were then incubated overnight at 4°C with antibodies against phosphorylated VEGFR-2 (p-VEGFR-2) at Y1175 (1:1000; #3770; Cell Signaling Technology, Beverly, MA) or phosphorylated ERK 1/2 (p-ERK 1/2) at T202/Y204 (1:2000; #9106; Cell Signaling Technology). Goat anti-mouse or goat anti-rabbit horse-radish-peroxidase (HRP)-conjugated antibodies (1:2000; Rockland Immunochemicals, Limerick, PA) were incubated for 1 h at room temperature. After the addition of SuperSignal™ chemiluminescent substrate (Thermo Fisher Scientific), blots were imaged using a FujiFilm ImageQuant LAS-4000 (FujiFilm Life Science). Following imaging, membranes were stripped with Restore Stripping Buffer (Thermo Fisher Scientific), re-blocked, and probed with antibodies against total VEGFR-2 (1:1000; #sc-6251; Santa Cruz Biotechnology, Santa Cruz, CA) or total ERK 1/2 (1:1000; #9102; Cell Signaling Technology) followed by goat anti-mouse or goat anti-rabbit HRP-conjugated secondary antibodies (1:2000; Rockland Immunochemicals). Lastly, α-tubulin (1:20,000; #05-829; Millipore, Billerica, MA) was stained as a loading control. Densitometry analysis was performed in ImageJ.

VEGFR-2 Immunofluorescence and Analysis

HUVECs were pretreated with Y-27632 (5 μM; BioVision, Milpitas, CA) or DMSO vehicle (Sigma-Aldrich) for 12 h. Cells were stimulated with 5 ng/ml VEGF (R&D Systems) for 15 min, rinsed with PBS, and then immediately fixed with 3.2% v/v paraformaldehyde (Electron Microscopy Systems, Hatfield, PA) for 10 min. After being washed with 0.02% v/v Tween (JT Baker) in PBS, HUVECs were permeabilized with 0.1% v/v Triton X-100 (JT Baker) in PBS with 5% v/v donkey serum (Millipore) for 20 min. Cells were blocked in 5% v/v donkey serum (Millipore) in PBS for 1 h and then incubated with VEGFR-2 antibody (1:50; #ab9530; Abcam, Cambridge, MA) in 0.01% v/v Triton X-100 (JT Baker), 5% v/v donkey serum (Millipore) in PBS overnight at 4°C. Alexa Fluor 488 donkey anti-mouse antibody (1:200; Thermo Fisher Scientific) was incubated for 1 h. Nuclei were

counterstained with 4′,6-diamidino-2-phenylindole (DAPI; 1:500; Thermo Fisher Scientific). To image, gels were inverted onto a drop of Vectashield™ Mounting Media (Vector Laboratories, Burlingame, CA) placed on a thin coverslip (No. 1, 48x65 mm, Thermo Fisher Scientific). Fluorescent z-stack images of each sample were acquired with a 40x water-immersion objective on a Zeiss LSM 700 confocal microscope on a Zeiss Axio Observer Z1 inverted stand (Carl Zeiss, Oberkochen, Germany). Images are presented as maximum intensity projections of z-stacks, unless otherwise stated. For analysis, cells were outlined in ImageJ and mean fluorescence intensity was measured. Additionally, the average number and size of VEGFR-2 clusters was calculated in ImageJ by thresholding images, analyzing particles, and normalizing per nucleus.

Colocalization of VEGFR-2 with EEA-1

Sub-confluent HUVECs were seeded on 1 and 10 kPa collagen-coated gels. One day post seeding, cells were pretreated with 5 μM Y-27632 (BioVision) or DMSO vehicle (Sigma-Aldrich) for 12 h. Following 15 min VEGF (R&D Systems) incubation, cells were fixed and co-stained with VEGFR-2 primary antibody (1:50; #ab9530; Abcam) and early endosomal antigen-1 (EEA-1) primary antibody (1:50; #ab2900; Abcam) as described above. Alexa Fluor 488 donkey anti-mouse and Alexa Fluor 568 donkey anti-rabbit secondary antibodies (1:200; Thermo Fisher Scientific) were utilized. Cells were counterstained with DAPI (1:500; Thermo Fisher Scientific) to visualize nuclei. Gels were inverted onto glass coverslips and a z-stack image of each sample was captured using a Zeiss LSM 700 confocal microscope equipped with a 40x water-immersion objective. Analysis was performed utilizing a custom-written Matlab code previously described [23] with slight modifications. Briefly, VEGFR-2 and EEA-1 z-stack images were converted into image sequences in ImageJ. In Matlab, image sequences were subjected to an adaptive Weiner filter (0.78 μm filtering window) to remove background noise, then image sections with structures presenting a signal-to-noise ratio greater than 2:1 were subjected to a top-hat filter (0.78 μm diameter disc). A median filter (0.63 μm filtering window) was applied to correct for variations in intensity. VEGFR-2 and EEA-1 colocalization was quantified by overlaying corresponding VEGFR-2 and EEA-1 filtered images to generate a 3D overlapping volume data. The number of colocalization events for each image was then normalized per cell.

Surface-Bound VEGFR-2 Immunofluorescence

Sub-confluent HUVECs were pretreated with 5 μM Y-27632 (BioVision) or DMSO vehicle (Sigma-Aldrich) for 12 h and then stimulated with 5 ng/ml VEGF (R&D Systems) for 15 min. Cells were fixed and stained with VEGFR-2 (1:50; #ab9530; Abcam) as described above, however, omitting cell permeabilization with Triton X-100 and wash steps involving Tween to visualize only membrane-bound VEGFR-2. Nuclei were counterstained with DAPI (1:500; Thermo Fisher Scientific). Fluorescent images were captured with a 40x water-immersion objective on a Zeiss LSM 700 confocal microscope. The number of VEGFR-2 clusters on the cell surface was calculated in ImageJ as described previously, and reported per cell.

Proliferation Assay

One day post seeding, sub-confluent HUVECs were serum starved in EBM (Lonza) for 24 h. PD98059 (10 or 20 μM; Cell Signaling Technology) or DMSO vehicle (Sigma-Aldrich) was added to the cells for the final hour of serum starving. Cells were stimulated with 5 ng/ml VEGF (R&D Systems) in 0.1% v/v FBS in EBM for 20 h. 10 μM 5-ethynyl-2′-deoxyuridine (EdU; Thermo Fisher Scientific) was added for 4 h and cells were fixed with 3.7% v/v formaldehyde (Alfa Aesar, Ward Hill, MA) for 15 min. HUVECs were stained with the Click-iT EdU Kit (Thermo Fisher Scientific) following the manufacturer's instructions and nuclei were counterstained with DAPI (Thermo Fisher Scientific). Cells were imaged with a 10x objective on a Zeiss Axio Observer Z1 inverted phase-contrast microscope (Carl Zeiss) with a Hamamatsu ORCA-ER camera. The percentage of EdU incorporation was calculated as the ratio of EdU positive cells to the total number of cells. Cell counts from 15 representative fields of view are also reported.

Actin Stress Fiber Immunofluorescence

Sub-confluent HUVECs seeded on collagen-coated 1 and 10 kPa PA gels were stimulated with 5 ng/ml VEGF (R&D Systems) for 15 min and then fixed with 3.7% v/v formaldehyde (Alfa Aesar) for 10 min. Cells were washed with 0.02% v/v Tween (JT Baker) in PBS and permeabilized for 5 min with 1% v/v Triton X-100 (JT Baker) in PBS before being incubated with Alexa Fluor 488 phalloidin (1:100; Thermo Fisher Scientific) and DAPI (1:500; Thermo Fisher Scientific) for 30 min at room temperature. Fluorescent z-stack images were obtained with a Zeiss LSM 700 confocal microscope on a Zeiss Axio Observer Z1 inverted stand (Carl Zeiss) equipped with a 40x water-immersion objective. The average number of stress fibers per cell was quantified using the ImageJ Tubeness plugin, as described previously [41].

Statistical Analysis

All analyses were performed using GraphPad Prism 7 (GraphPad Software, La Jolla, CA) or Excel 2016 (Microsoft, Redmond, WA). Where appropriate, student's *t*-tests or parametric one-way or two-way ANOVAs with post hoc Tukey's honest significant difference test were performed. $P < 0.05$ was considered statistically significant. All values are presented as mean ± standard error (SE).

Results

Matrix stiffness enhances VEGF-induced VEGFR-2 response in sub-confluent endothelial monolayers

To investigate the interplay of signaling pathways activated by both VEGF and ECM stiffness, we first probed VEGFR-2 activation. To represent healthy blood vessels, sub-confluent HUVECs were cultured on 1 kPa PA substrates [42]. Since matrix stiffening occurs during tumor progression [10,11], 10 kPa gels were utilized to mimic tumor tissue. After HUVECs were seeded onto 1 and 10 kPa gels and subjected to 5 min of 5 ng/ml VEGF stimulation, activated VEGFR-2 levels (ratio of Y1175 phosphorylated VEGFR-2 (p-VEGFR-2) to total VEGFR-2) was significantly increased on stiffer matrices (Figure 1A–

B,D–E). This response was independent of whether the cells were cultured on collagen-coated (Figure 1A–C) or fibronectin-coated (Figure 1D–F) matrices, although the magnitude of the response was much more robust for cells cultured on collagen. Interestingly, no changes were observed in the level of p-VEGFR-2 relative to the housekeeping gene α-tubulin (Figure 1C,F), demonstrating no stiffness-mediated changes in the level of p-VEGFR-2 in HUVECs.

Next, we investigated VEGFR-2 expression with and without VEGF simulation as a function of ECM stiffness. Sub-confluent cells on stiffer substrates had significantly less VEGFR-2 compared to compliant matrices both without VEGF treatment (control) and after 15 min VEGF treatment (VEGF; Figure 2A–B). Additionally, we observed a decrease in VEGFR-2 expression after 15 min for both stiffness values tested (Figure 2A–B). However, the fold decrease in VEGFR-2 levels after stimulation with VEGF (VEGF/control) was independent of ECM stiffness (Figure 2B). These results confirm the findings of Mammoto et al. [15] which demonstrated that matrix stiffness modulates VEGF-independent VEGFR-2 expression in endothelial cells cultured on fibronectin-coated PA substrates and further suggest a decrease in VEGFR-2 following VEGF stimulation.

The addition of VEGF to endothelial cells rapidly initiates VEGFR-2 endocytosis, an important step in downstream VEGF signaling [43,44]. Since endocytosis in stem cells can be influenced by matrix stiffness [45], we sought to determine the effect of stiffness on VEGF-stimulated VEGFR-2 endocytosis in endothelial cells. Cells cultured on 1 and 10 kPa collagen-coated PA gels were subjected to 15 min VEGF stimulation, fixed, and immunostained for VEGFR-2 (Figure 2C). Indeed, total fluorescent intensity of VEGFR-2 significantly decreased with increasing matrix stiffness (Figure 2D). Total fluorescent intensity of VEGFR-2 also decreased following VEGF stimulation at each stiffness (Figure 2D). Moreover, VEGF treatment induced VEGFR-2 clustering (Figure 2C, arrows), where the average size of VEGFR-2 clusters increased with VEGF stimulation regardless of ECM stiffness (Figure 2E), suggesting receptor aggregation and packaging for endocytosis [43]. VEGFR-2 clusters were more numerous and larger in size following VEGF treatment in cells on more compliant substrates compared to cells on stiffer substrates (Figure 2E–F). The fold change in VEGFR-2 cluster size, but not intensity or cluster number, from the addition of VEGF (VEGF/control) increased on stiff matrices compared to compliant substrates (Figure S1), indicating stiffness increased cluster size in response to VEGF but not the number or intensity of clusters. Since matrix stiffness has been shown to regulate cell behavior and signaling via the Rho/ROCK pathway [22,30], we also investigated its role in VEGFR-2 localization and clustering. Pretreatment of HUVECs on 10 kPa gels with Y-27632, a ROCK inhibitor [46], abrogated the reduced VEGFR-2 signal, cluster size, and cluster number compared to untreated cells on stiff substrates (Figure 2C–F). Cells on stiff substrates that were treated with Y-27632 exhibited VEGFR-2 clustering that resembled the clustering seen on more compliant matrices.

To further investigate the role of matrix stiffness on VEGFR-2 trafficking within our system, we probed VEGFR-2 colocalization with an early endosomal marker, early endosomal antigen-1 (EEA-1) [44,47]. Sub-confluent endothelial cells cultured on compliant and stiff collagen-coated gels were stimulated with VEGF for 15 min, fixed, and immunostained for

VEGFR-2 and EEA-1 (Figure 3A). In the absence of VEGF stimulation (control), a significant increase in VEGFR-2 colocalization with EEA-1 was observed in cells seeded on stiff matrices (Figure 3B), indicating increased VEGFR-2 internalization on stiff substrates. Furthermore, after stimulation with VEGF, VEGFR-2 and EEA-1 colocalization increased further (Figure 3B), indicating rapid VEGF-induced VEGFR-2 endocytosis. However, the fold change in VEGFR-2 and EEA-1 colocalization with without VEGF treatment (control) compared to VEGF treatment was independent of matrix stiffness (Figure S2A). In addition, VEGFR-2 levels on the cell membrane were measured in non-permeabilized cells under all conditions (Figure 3C). As expected, decreased levels of cell surface-bound VEGFR-2 were observed as a function of ECM stiffness and VEGF treatment (Figure 3D), correlating with an increase in VEGFR-2 and EEA-1 colocalization (Figure 3B). The fold change due to VEGF stimulation was not significantly different between any conditions (Figure S2B) revealing no difference in VEGF responsiveness with stiffness, but that changes in receptor internalization are stiffness-mediated regardless of treatment. Since Rho/ROCK signaling affected receptor clustering (Figure 2), we investigated the role of Rho/ROCK signaling in VEGFR-2 internalization. Cells were cultured on 10 kPa gels and pretreated with Y-27632 before exposure to 15 min VEGF stimulation. Inhibiting ROCK reduced VEGFR-2 colocalization with EEA-1 (Figure 3B), indicating reduced receptor internalization and increased VEGFR-2 remaining on the cell surface. However, the levels were still significantly lower than those in cells cultured on 1 kPa gels (Figure 3D). Together, these data suggest a vital role of matrix mechanics in VEGFR-2 endocytosis and trafficking in endothelial cells.

It has previously been shown that VEGFR-2 is negatively regulated at cell-cell junctions to maintain contact inhibition and prevent VEGF-induced overproliferation [47,48]. Therefore, we investigated the influence of matrix stiffness on VEGFR-2 signaling in a confluent monolayer. HUVECs were seeded on 1 and 10 kPa gels and grown to full confluence before stimulating with 5 ng/ml VEGF. Interestingly, VEGFR-2 phosphorylation and total VEGFR-2 levels did not differ with increased matrix stiffness (Figure 4A–D) as seen in sub-confluent cells (Figure 1,2), indicating that the effects of matrix stiffness on activated and total VEGFR-2 levels following VEGF stimulation are sensitive to monolayer confluence.

Matrix mechanics regulate VEGF-mediated ERK 1/2 signaling and proliferation in sub-confluent cells

Given our results indicating that matrix stiffness alters VEGFR-2 activation in sub-confluent endothelial cells, we investigated its effects on downstream signals and proliferation as a phenotypic output. ERK 1/2 is a common downstream effector molecule activated by both VEGF and matrix stiffness pathways [9,14], and VEGF promotes endothelial proliferation [48–55] in an ERK-dependent manner [9,52]. We cultured HUVECs on soft and stiff PA gels to 50–70% confluence. When stimulated with 5 ng/ml VEGF, ERK 1/2 phosphorylation increased on stiff substrates after 5 min to a greater extent than the activation detected on compliant substrates (Figure 5A–C). Since ERK signaling mediates proliferation, S-phase cells were labelled and enumerated after 24 h VEGF treatment to determine whether proliferation is affected. Quantification of the percentage of proliferating (EdU positive) cells revealed that, without any exogenous VEGF added, HUVECs displayed a 2.4-fold

increase in proliferation on stiffer gels compared to more compliant matrices (Figure 5D). In addition, proliferation increased more than two-fold on both compliant and stiff matrices following 5 ng/ml VEGF treatment (Figure 5D). Preincubation of cells with PD98059, an ERK 1/2 inhibitor, significantly decreased proliferation of endothelial cells cultured on both compliant and stiff substrates in a dose-dependent manner (Figure 5D). Similarly, a 3.5-fold increase in cell count was observed with increasing stiffness without VEGF treatment (Figure 5E). With VEGF stimulation cell numbers significantly increased, but PD98059 pretreatment diminished this effect (Figure 5E). To test if the increase observed in cell proliferation for HUVECs on 10 kPa gels following VEGF stimulation was a result of synergism between the individual stimuli, the response was compared to the sum of the response magnitude for stiffness and VEGF separately. Our results indicate that the combined effect of increasing matrix stiffness and adding VEGF simultaneously was not greater than the sum of the responses from each individual cue (Figure 5D–E), suggesting a complex interaction of these pathways on endothelial proliferation rate and cell counts.

After observing differential VEGFR-2 signaling in sub-confluent compared to confluent cells (Figures 1,4), we investigated the effect of confluency on ERK 1/2. HUVECs were seeded on 1 or 10 kPa gels and grown to confluence. When probed for ERK 1/2 phosphorylation and total ERK 1/2 levels in response to VEGF stimulation, we did not detect a change in ERK 1/2 signal as a function of matrix stiffness (Figure 6A–D), unlike the response we observed in sub-confluent cells (Figure 5A–B). These data suggest that the VEGF-induced response of both VEGFR-2 and ERK 1/2 is dependent upon monolayer confluency.

Matrix stiffness and VEGF stimulate actin stress fiber formation in endothelial cells

VEGF has been shown to induce the formation of actin stress fibers in endothelial cells cultured on glass or plastic [56,57]. To investigate the role of matrix stiffness in VEGF-mediated stress fiber formation, sub-confluent endothelial monolayers seeded on 1 and 10 kPa gels were subjected to 5 ng/ml VEGF stimulation for 15 min, fixed, and stained for actin (Figure 7A). Quantification of control conditions revealed a more than three-fold increase in the number of stress fibers per cell on stiffer gels compared to more compliant substrates (Figure 7B), as has been previously observed [58]. Moreover, adding VEGF increased the actin intensity (Figure 7A) as well as increased the number of fibers more than 1.3-fold for each gel stiffness (Figure 7B). Together, HUVECs on stiff gels with VEGF treatment displayed over a fourfold increase in the number of stress fibers compared to cells on compliant substrates without VEGF stimulation (Figure 7B). While comparing the increase in stress fiber formation due to stiffness with the increase in stress fiber formation due to VEGF, our results indicate that the effects of both stiffness and VEGF were approximately additive (Figure 7B), suggesting a complementary, non-competitive enhancement from each signaling pathway.

Discussion

Since VEGF signaling and altered matrix mechanics are both integral parts of tumor progression, specifically tumor angiogenesis, and signal through similar pathways, we

sought to study their cooperative effects on endothelial cell behavior. Our data indicate that ECM stiffness increases VEGFR-2 internalization, which heightens downstream VEGF response and signaling, specifically ERK 1/2 phosphorylation, cell proliferation, and the formation of actin stress fibers, in sub-confluent endothelial cells.

Matrix stiffness is an important regulator of endothelial cell behavior [13,16–27] and more recently, matrix mechanics have also been shown to alter protein expression [15,16,31,59]. Importantly, Mammoto et al. [15] observed that increasing ECM stiffness elicits a VEGF-independent, biphasic response in VEGFR-2 levels due to stiffness-mediated regulation of VEGFR-2 transcription factors. In the present study, we also found that VEGFR-2 levels are sensitive to matrix stiffness in HUVECs, further supporting stiffness-mediated control of receptor expression. We observed different levels of VEGFR-2 phosphorylation to total VEGFR-2 with stiffness, but we would not expect complete receptor occupancy to occur with the conditions in our system [60–62]. Notably, we did not observe changes in VEGFR-2 phosphorylation levels as a function of matrix stiffness compared to the total cellular protein content. This finding suggests that ECM compliance does not influence VEGFR-2 responsiveness to VEGF stimulation. However, at increased levels of VEGF treatment where complete receptor occupancy occurs at each matrix stiffness, different response and signaling may be observed.

VEGF stimulation promotes VEGFR-2 endocytosis [43,44], and our data also indicate increased VEGFR-2 clustering and decreased total VEGFR-2 levels following VEGF treatment. This correlates with increased VEGFR-2 colocalization with EEA-1 and reduced surface-bound VEGFR-2 levels. However, no significant change in response to VEGF treatment was observed with changes in matrix stiffness. Interestingly, in the absence of exogenous stimuli, we did detect significantly increased VEGFR-2 internalization in cells cultured on stiff matrices compared to compliant substrates, as well as elevated downstream signaling, cell proliferation, and actin stress fiber formation following VEGF treatment. Together, these findings demonstrate that changes in receptor internalization are VEGF-independent but stiffness-mediated.

It is known that matrix stiffening influences cell contractility via Rho/ROCK signaling [22,63]. Elevated Rho activity is observed in endothelial cells cultured on stiff substrates compared to compliant matrices [22,23] and inhibiting ROCK with Y-27632 treatment reduces endothelial cell contractility [22]. Previously, others have probed the interactions of signaling pathways involving VEGF and Rho/ROCK and found that VEGF induces Rho activation [27,57] and its membrane recruitment [57]. Y-27632 pretreatment disrupts VEGF-induced endothelial cell migration [27,57], angiogenesis [27], and permeability [27]. Here, we show an additional role of Rho/ROCK signaling in VEGF-independent VEGFR-2 clustering and internalization. We demonstrate that increased matrix stiffness decreased VEGFR-2 intensity, cluster size, and cluster number compared to compliant matrices, suggesting more VEGFR-2 clusters are endocytosed on stiff substrates. Indeed, matrix stiffness also significantly increased VEGFR-2 and EEA-1 colocalization, indicating elevated VEGFR-2 internalization. These results suggest that VEGFR-2 internalization is more active on stiff substrates compared to compliant matrices. Since internalization is required for many downstream VEGF signaling events including ERK 1/2 phosphorylation

[9,44], increased internalization provides a possible explanation for enhanced proliferation and behavior, such as the formation of stress fibers seen on stiff substrates following VEGF treatment. Notably, Y-27632 treatment abrogated the stiffness-mediated decrease in VEGFR-2 intensity, cluster size, and cluster number initially observed in endothelial cells on stiff substrates, as well as VEGFR-2 packaging into EEA-1-positive endocytic vesicles in endothelial cells. Together, our data indicate that, even in the absence of exogenous VEGF ligand, Rho/ROCK signaling is at least partially involved in the stiffness-mediated changes in VEGFR-2 internalization and downstream signaling we observe. This suggests that increased Rho/ROCK signaling could modify or enhance the molecular interactions of VEGFR-2 with integrins or other associated intracellular signaling molecules, resulting in altered VEGF-stimulated endocytosis and downstream signaling.

However, others have observed decreased VEGFR-2 internalization in bovine aortic endothelial cells cultured on compliant substrates [37]. Strikingly, this study observed reduced β1 integrin activation with increasing matrix stiffness, whereas many others report heightened integrin activation and signaling as a function of ECM stiffness [10,14,42,64], which could contribute to the differences in results. Utilizing a different gel system and endothelial cell type, our data show that HUVECs display enhanced VEGFR-2 internalization and VEGF-stimulated downstream signaling with elevated matrix stiffness.

Matrix stiffness is known to promote Rho-mediated endothelial proliferation [58,65,66]. In agreement with other studies, we report elevated proliferation of sub-confluent endothelial cells cultured on stiff substrates compared to compliant matrices without VEGF treatment, which was reduced by inhibiting ERK 1/2. VEGF has also been shown to stimulate endothelial proliferation [48–55], primarily mediated though VEGFR-2 signaling [9]. While integrating multiple cues, our results indicate increased ERK 1/2 activation and proliferation in endothelial cells on stiff matrices following VEGF treatment. PD98059, an ERK 1/2 inhibitor, has previously been shown to inhibit VEGF-induced proliferation of HUVECs [49–51] and other endothelial cell types [48,52,53] cultured on glass or plastic. Further, our data demonstrate that PD98059 treatment reduced proliferation following VEGF stimulation of endothelial cells cultured on both compliant and stiff substrates. Since VEGFR-2 is internalized prior to ERK 1/2 activation [9,44], our data suggests that increased matrix stiffness promotes VEGFR-2 internalization, resulting in elevated ERK 1/2 phosphorylation and cell proliferation. Together, this suggests that aberrant Rho/ROCK signaling in the tumor microenvironment may modify the normal interaction between Rho/ROCK and ERK 1/2 pathways during healthy angiogenesis [66] to promote sustained ERK 1/2 activation [67], resulting in elevated proliferation during cancer.

Another downstream response to VEGF stimulation in endothelial cells is the formation of actin stress fibers. Cells form actin stress fibers when they encounter a mechanical force, and their formation is essential to cell adhesion and migration. As such, we also investigated changes in the cytoskeleton and actin stress fiber formation at different matrix stiffness to evaluate the role of matrix mechanics in VEGF-induced signaling. Previously, Yeh and colleagues [58] observed increased actin intensity in endothelial cells cultured on stiff gels compared to compliant matrices. Our data further support stiffness-enhanced fiber formation without VEGF treatment and quantify the average number of stress fibers per cell.

Additionally, VEGF stimulation triggers stress fiber formation in endothelial cells within our system and others [56,57]. Since stress fiber formation also requires VEGFR-2 internalization, this suggests that cells cultured on stiffer substrates display an enhanced number of fibers due to more receptor internalization compared to compliant substrates.

Previously, others have also observed changes in intracellular signaling [68–72] and cell morphology and behavior [48,73,74] as monolayers reach confluence. Importantly, the relationship between VE-cadherin, an adherens junctional protein whose activity is highly upregulated as endothelial cells establish cell-cell contacts [75], and VEGFR-2 has been studied extensively [47,48,76,77]. In the absence of a stimulus, VE-cadherin binds VEGFR-2 to reinforce its inactive state [8] while being continuously endocytosed and recycled back to the membrane [78]. With the addition of VEGF to sub-confluent endothelial cells, VE-cadherin is phosphorylated and endocytosed to downregulate its activity, allowing VEGFR-2 activation [76,77]. Upon reaching confluence, VE-cadherin inhibits VEGF-stimulated endothelial proliferation by associating with VEGFR-2, dramatically decreasing its internalization and signaling [47,48]. In the present study, we did not observe stiffness-enhanced signaling in confluent cells, suggesting that matrix stiffening does not overcome the negative regulation from VE-cadherin in our system.

Conclusions

The individual impacts of VEGF and matrix stiffness on endothelial behavior have been previously investigated, however their concerted efforts are less well understood. Here, we show enhanced VEGFR-2 endocytosis and downstream VEGF-induced ERK 1/2 signaling, cell proliferation, and formation of stress fibers in endothelial cells cultured on stiffer substrates. This work helps to provide a possible mechanism to explain several observations about stiffness-mediated activation of growth factor receptors. Importantly, identifying mechanistic crosstalk and subsequent behavioral effects may aid in developing therapeutics to combat their dysregulation during diseases such as cancer.

Supplementary Material

Refer to Web version on PubMed Central for supplementary material.

Acknowledgments

This work was supported by grants from the National Institute of Health (R01HL127499) to C.A.R.-K., a scholarship for the Next Generation of Scientist from the Cancer Society to F.B., and the National Science Foundation Graduate Research Fellowship Program to D.J.L. and M.R.Z.

References

1. Carmeliet P, Jain RK. Angiogenesis in cancer and other diseases. Nature. 2000; 407:249–57. [PubMed: 11001068]
2. Fukumura D, Jain RK. Tumor microenvironment abnormalities: causes, consequences, and strategies to normalize. J Cell Biochem. 2007; 101:937–49. [PubMed: 17171643]
3. Chauhan VP, Stylianopoulos T, Boucher Y, Jain RK. Delivery of molecular and nanoscale medicine to tumors: transport barriers and strategies. Annu Rev Chem Biomol Eng. 2011; 2:281–98. [PubMed: 22432620]

4. Jain RK. Normalization of tumor vasculature: an emerging concept in antiangiogenic therapy. Science. 2005; 307:58–62. [PubMed: 15637262]
5. Ferrara N, Davis-Smyth T. The biology of vascular endothelial growth factor. Endocr Rev. 1997; 18:4–25. [PubMed: 9034784]
6. Senger DR, Galli SJ, Dvorak AM, Perruzzi CA, Harvey VS, Dvorak HF. Tumor cells secrete a vascular permeability factor that promotes accumulation of ascites fluid. Science. 1983; 219:983–5. [PubMed: 6823562]
7. Carmeliet P, Jain RK. Molecular mechanisms and clinical applications of angiogenesis. Nature. 2011; 473:298–307. [PubMed: 21593862]
8. Simons M, Gordon E, Claesson-Welsh L. Mechanisms and regulation of endothelial VEGF receptor signalling. Nat Rev Mol Cell Biol. 2016; 17:611–25. [PubMed: 27461391]
9. Holmes K, Roberts OL, Thomas AM, Cross MJ. Vascular endothelial growth factor receptor-2: structure, function, intracellular signalling and therapeutic inhibition. Cell Signal. 2007; 19:2003–12. [PubMed: 17658244]
10. Levental KR, et al. Matrix crosslinking forces tumor progression by enhancing integrin signaling. Cell. 2009; 139:891–906. [PubMed: 19931152]
11. Lopez JI, Kang I, You W-K, McDonald DM, Weaver VM. In situ force mapping of mammary gland transformation. Integr Biol. 2011; 3:910–21.
12. Discher DE, Janmey P, Wang Y-L. Tissue cells feel and respond to the stiffness of their substrate. Science. 2005; 310:1139–43. [PubMed: 16293750]
13. LaValley DJ, Reinhart-King CA. Matrix stiffening in the formation of blood vessels. Adv Regen Biol. 2014; 1:25247.
14. Huveneers S, Danen EHJ. Adhesion signaling - crosstalk between integrins, Src and Rho. J Cell Sci. 2009; 122:1059–69. [PubMed: 19339545]
15. Mammoto A, Connor KM, Mammoto T, Yung CW, Huh D, Aderman CM, Mostoslavsky G, Smith LEH, Ingber DE. A mechanosensitive transcriptional mechanism that controls angiogenesis. Nature. 2009; 457:1103–8. [PubMed: 19242469]
16. Bordeleau F, Califano JP, Abril YLN, Mason BN, LaValley DJ, Shin SJ, Weiss RS, Reinhart-King CA. Tissue stiffness regulates serine/arginine-rich protein-mediated splicing of the extra domain B-fibronectin isoform in tumors. Proc Natl Acad Sci. 2015; 112:8314–9. [PubMed: 26106154]
17. Deroanne CF, Lapiere CM, Nusgens BV. In vitro tubulogenesis of endothelial cells by relaxation of the coupling extracellular matrix-cytoskeleton. Cardiovasc Res. 2001; 49:647–58. [PubMed: 11166278]
18. Califano JP, Reinhart-King CA. A balance of substrate mechanics and matrix chemistry regulates endothelial cell network assembly. Cell Mol Bioeng. 2008; 1:122–32.
19. Shamloo A, Heilshorn SC. Matrix density mediates polarization and lumen formation of endothelial sprouts in VEGF gradients. Lab Chip. 2010; 10:3061–8. [PubMed: 20820484]
20. Wu Y, Al-Ameen MA, Ghosh. Integrated effects of matrix mechanics and vascular endothelial growth factor (VEGF) on capillary sprouting. Ann Biomed Eng. 2014; 42:1024–36. [PubMed: 24558074]
21. Mason BN, Starchenko A, Williams RM, Bonassar LJ, Reinhart-King CA. Tuning three-dimensional collagen matrix stiffness independently of collagen concentration modulates endothelial cell behavior. Acta Biomater. 2013; 9:4635–44. [PubMed: 22902816]
22. Huynh J, Nishimura N, Rana K, Peloquin JM, Califano JP, Montague CR, King MR, Schaffer CB, Reinhart-King CA. Age-related intimal stiffening enhances endothelial permeability and leukocyte transmigration. Sci Transl Med. 2011; 3:112ra122.
23. Lampi MC, Faber CJ, Huynh J, Bordeleau F, Zanotelli MR, Reinhart-King CA. Simvastatin ameliorates matrix stiffness-mediated endothelial monolayer disruption. PLoS One. 2016; 11:e0147033. [PubMed: 26761203]
24. Urbano RL, Furia C, Basehore S, Clyne AM. Stiff substrates increase inflammation-induced endothelial monolayer tension and permeability. Biophys J. 2017; 3:645–55.
25. Mammoto A, Mammoto T, Kanapathipillai M, Wing Yung C, Jiang E, Jiang A, Lofgren K, Gee EPS, Ingber DE. Control of lung vascular permeability and endotoxin-induced pulmonary oedema by changes in extracellular matrix mechanics. Nat Commun. 2013; 4:1759. [PubMed: 23612300]

26. Bordeleau F, et al. Matrix stiffening promotes a tumor vasculature phenotype. Proc Natl Acad Sci. 2016; 114:492–7. [PubMed: 28034921]
27. Bryan BA, Dennstedt E, Mitchell DC, Walshe TE, Noma K, Loureiro R, Saint-Geniez M, Campaigniac J-P, Liao JK, D'Amore PA. RhoA/ROCK signaling is essential for multiple aspects of VEGF-mediated angiogenesis. FASEB J. 2010; 24:3186–95. [PubMed: 20400538]
28. Ingber DE. Mechanical signaling and the cellular response to extracellular matrix in angiogenesis and cardiovascular physiology. Circ Res. 2002; 91:877–87. [PubMed: 12433832]
29. van Oers RFM, Rens EG, LaValley DJ, Reinhart-King CA, Merks RMH. Mechanical cell-matrix feedback explains pairwise and collective endothelial cell behavior in vitro. PLoS Comput Biol. 2014; 10:e1003774. [PubMed: 25121971]
30. Paszek MJ, et al. Tensional homeostasis and the malignant phenotype. Cancer Cell. 2005; 8:241–54. [PubMed: 16169468]
31. Leight JL, Wozniak MA, Chen S, Lynch ML, Chen CS. Matrix rigidity regulates a switch between TGF-B1-induced apoptosis and epithelial-mesenchymal transition. Mol Biol Cell. 2012; 23:781–91. [PubMed: 22238361]
32. Kim J-H, Asthagiri AR. Matrix stiffening sensitizes epithelial cells to EGF and enables the loss of contact inhibition of proliferation. J Cell Sci. 2011; 124:1280–7. [PubMed: 21429934]
33. Brown XQ, Bartolak-Suki E, Williams C, Walker ML, Weaver VM, Wong JY. Effect of substrate stiffness and PDGF on the behavior of vascular smooth muscle cells: implications for atherosclerosis. J Cell Physiol. 2010; 225:115–22. [PubMed: 20648629]
34. Huynh J, Bordeleau F, Kraning-Rush CM, Reinhart-King CA. Substrate stiffness regulates PDGF-induced circular dorsal ruffle formation through MLCK. Cell Mol Bioeng. 2013; 6:138–47.
35. Hanjaya-Putra D, Yee J, Ceci D, Truitt R, Yee D, Gerecht S. Vascular endothelial growth factor and substrate mechanics regulate in vitro tubulogenesis of endothelial progenitor cells. J Cell Mol Med. 2010; 14:2436–47. [PubMed: 19968735]
36. Wingate K, Floren M, Tan Y, Tseng PON, Tan W. Synergism of matrix stiffness and vascular endothelial growth factor on mesenchymal stem cells for vascular endothelial regeneration. Tissue Eng Part A. 2014; 20:2503–12. [PubMed: 24702044]
37. Sack KD, Teran M, Nugent MA. Extracellular matrix stiffness controls VEGF signaling and processing in endothelial cells. J Cell Physiol. 2016; 9999:1–14.
38. Reinhart-King CA, Dembo M, Hammer DA. Endothelial cell traction forces on RGD-derivatized polyacrylamide substrata. Langmuir. 2003; 19:1573–9.
39. Peloquin J, Huynh J, Williams RM, Reinhart-King CA. Indentation measurements of the subendothelial matrix in bovine carotid arteries. J Biomech. 2011; 44:815–21. [PubMed: 21288524]
40. Gallagher, SR. Current Protocols in Cell Biology: Electrophoresis and Immunoblotting. Bonifacino, JS., et al., editors. Bethesda, MD: John Wiley & Sons, Inc; 2007. p. 6.1.31
41. Bordeleau F, Lapierre M-EM, Sheng Y, Marceau N. Keratin 8/18 regulation of cell stiffness-extracellular matrix interplay through modulation of Rho-mediated actin cytoskeleton dynamics. PLoS One. 2012; 6:e38780.
42. Butcher DT, Alliston T, Weaver VM. A tense situation: forcing tumour progression. Nat Rev Cancer. 2009; 9:108–22. [PubMed: 19165226]
43. Nakayama M, et al. Spatial regulation of VEGF receptor endocytosis in angiogenesis. Nat Cell Biol. 2013; 15:249–60. [PubMed: 23354168]
44. Simons M. An Inside View: VEGF Receptor Trafficking and Signaling. Physiol Rev. 2012; 27:213–22.
45. Du J, Chen X, Liang X, Zhang G, Xu J, He L, Zhan Q, Feng X-Q, Chien S, Yang C. Integrin activation and internalization on soft ECM as a mechanism of induction of stem cell differentiation by ECM elasticity. Proc Natl Acad Sci. 2011; 108:9466–71. [PubMed: 21593411]
46. Ishizaki T, Uehata M, Tamechika I, Keel J, Nonomura K, Maekawa M, Narumiya S. Pharmacological properties of Y-27632, a specific inhibitor of Rho-associated kinases. Mol Pharmacol. 2000; 57:976–83. [PubMed: 10779382]

47. Lampugnani MG, Orsenigo F, Gagliani MC, Tacchetti C, Dejana E. Vascular endothelial cadherin controls VEGFR-2 internalization and signaling from intracellular compartments. J Cell Biol. 2006; 174:593–604. [PubMed: 16893970]
48. Lampugnani MG, et al. Contact inhibition of VEGF-induced proliferation requires vascular endothelial cadherin, B-catenin, and the phosphatase DEP-1/CD148. J Cell Biol. 2003; 161:793–804. [PubMed: 12771128]
49. Zeng H, Dvorak HF, Mukhopadhyay D. Vascular permeability factor (VPF)/vascular endothelial growth factor (VEGF) receptor-1 down-modulates VPF/VEGF receptor-2-mediated endothelial cell proliferation, but not migration, through phosphatidylinositol 3-kinase-dependent pathways. J Biol Chem. 2001; 276:26969–79. [PubMed: 11350975]
50. Kanno S, Oda N, Abe M, Terai Y, Ito M, Shitara K, Tabayashi K, Shibuya M, Sato Y. Roles of two VEGF receptors, Flt-1 and KDR, in the signal transduction of VEGF effects in human vascular endothelial cells. Oncogene. 2000; 19:2138–46. [PubMed: 10815805]
51. Ali N, Yoshizumi M, Fujita Y, Izawa Y, Kanematsu Y, Ishizawa K, Tsuchiya K, Yano S, Sone S, Tamaki T. A novel src kinase inhibitor, M475271, inhibits VEGF-induced human umbilical vein endothelial cell proliferation and migration. J Pharmacol Sci. 2005; 98:130–41. [PubMed: 15937404]
52. Pedram A, Razandi M, Levin ER. Extracellular signal-regulated protein kinase/jun kinase cross-talk underlies vascular endothelial cell growth factor-induced endothelial cell proliferation. J Biol Chem. 1998; 273:26722–8. [PubMed: 9756915]
53. Kroll J, Waltenberger J. The vascular endothelial growth factor receptor KDR activates multiple signal transduction pathways in porcine aortic endothelial cells. J Biol Chem. 1997; 272:32521–7. [PubMed: 9405464]
54. Soker S, Gollamudi-Payne S, Fidder H, Charmahelli H, Klagsbrun M. Inhibition of vascular endothelial growth factor (VEGF) induced endothelial cell proliferation by a peptide corresponding to the exon-7 encoded domain of VEGF165. J Biol Chem. 1997; 272:31582–8. [PubMed: 9395496]
55. Yoshida A, Anand-apte B, Zetter BR. Differential endothelial migration and proliferation to basic fibroblast growth factor and vascular endothelial growth factor. Growth Factors. 1996; 13:57–64. [PubMed: 8962720]
56. Rousseau S, Houle F, Kotanides H, Witte L, Waltenberger J, Landry J, Huot J. Vascular endothelial growth factor (VEGF)-driven actin-based motility is mediated by VEGFR2 and requires concerted activation of stress-activated protein kinase 2 (SAPK2/p38) and geldanamycin-sensitive phosphorylation of focal adhesion kinase. J Biol Chem. 2000; 275:10661–72. [PubMed: 10744763]
57. van Nieuw Amerongen GP, Koolwijk P, Versteilen A, van Hinsbergh VW. Involvement of RhoA/Rho kinase signaling in VEGF-induced endothelial cell migration and angiogenesis in vitro. Arterioscler Thromb Vasc Biol. 2003; 23:211–7. [PubMed: 12588761]
58. Yeh Y-T, Hur SS, Chang J, Wang K-C, Chiu J-J, Li Y-S, Chien S. Matrix stiffness regulates endothelial cell proliferation through septin 9. PLoS One. 2012; 7:e46889. [PubMed: 23118862]
59. Mouw JK, et al. Tissue mechanics modulate microRNA-dependent PTEN expression to regulate malignant progression. Nat Med. 2014; 20:360–7. [PubMed: 24633304]
60. Mac Gabhann F, Popel AS, Mac Gabhann F, Popel AS, Mac Gabhann F, Popel AS. Model of competitive binding of vascular endothelial growth factor and placental growth factor to VEGF receptors on endothelial cells. Am J Physiol Circ Physiol. 2004; 286:H153–64.
61. Mac Gabhann F, Yang MT, Popel AS. Monte Carlo simulations of VEGF binding to cell surface receptors in vitro. Biochim Biophys Acta. 2005; 1746:95–107. [PubMed: 16257459]
62. Bentley K, Gerhardt H, Bates PA. Agent-based simulation of notch-mediated tip cell selection in angiogenic sprout initialisation. J Theor Biol. 2008; 250:25–36. [PubMed: 18028963]
63. Wang H-B, Dembo M, Wang Y-L. Substrate flexibility regulates growth and apoptosis of normal but not transformed cells. Am J Physiol Cell Physiol. 2000; 279:C1345–50. [PubMed: 11029281]
64. Delcommenne M, Streulis CH. Control of Integrin Expression by Extracellular Matrix. J Biol Chem. 1995; 270:26794–801. [PubMed: 7592919]

65. Provenzano PP, Keely PJ. Mechanical signaling through the cytoskeleton regulates cell proliferation by coordinated focal adhesion and Rho GTPase signaling. J Cell Sci. 124:1195–205.
66. Mavria G, Vercoulen Y, Yeo M, Paterson H, Karasarides M, Marais R, Bird D, Marshall CJ. ERK-MAPK signaling opposes Rho-kinase to promote endothelial cell survival and sprouting during angiogenesis. Cancer Cell. 2006; 9:33–44. [PubMed: 16413470]
67. Welsh CF, Roovers K, Villanueva J, Liu Y, Schwartz MA, Assoian RK. Timing of cyclin D1 expression within G1 phase is controlled by Rho. Nat Cell Biol. 2001; 3:950–7. [PubMed: 11715015]
68. Lampugnani MG, Corada M, Andriopoulou P, Esser S, Risau W, Dejana E. Cell confluence regulates tyrosine phosphorylation of adherens junction components in endothelial cells. J Cell Sci. 1997; 110:2065–77. [PubMed: 9378757]
69. Corvera S, DiBonaventura C, Shpetner HS. Cell confluence-dependent remodeling of endothelial membranes mediated by cholesterol. J Biol Chem. 2000; 275:31414–21. [PubMed: 10903311]
70. Jiang H, Weyrich AS, Zimmerman GA, McIntyre TM. Endothelial cell confluence regulates cyclooxygenase-2 and prostaglandin E2 production that modulate motility. J Biol Chem. 2004; 279:55905–13. [PubMed: 15485847]
71. Faust D, Dolado I, Cuadrado A, Oesch F, Weiss C, Nebreda AR, Dietrich C. p38alpha MAPK is required for contact inhibition. Oncogene. 2005; 24:7941–5. [PubMed: 16027723]
72. Curto M, Cole BK, Lallemand D, Liu CH, McClatchey AI. Contact-dependent inhibition of EGFR signaling by Nf2/Merlin. J Cell Biol. 2007; 177:893–903. [PubMed: 17548515]
73. Puliafito A, Hufnagel L, Neveu P, Streichan S, Sigal A, Fygenson DK, Shraiman BI. Collective and single cell behavior in epithelial contact inhibition. Proc Natl Acad Sci. 2012; 109:739–44. [PubMed: 22228306]
74. Ishibe S, Haydu JE, Togawa A, Marlier A, Cantley LG. Cell confluence regulates hepatocyte growth factor-stimulated cell morphogenesis in a B-catenin-dependent manner. Mol Cell Biol. 2006; 26:9232–43. [PubMed: 17030602]
75. Vestweber D. VE-cadherin: the major endothelial adhesion molecule controlling cellular junctions and blood vessel formation. Arterioscler Thromb Vasc Biol. 2008; 28:223–32. [PubMed: 18162609]
76. Esser S, Lampugnani M, Corada M, Dejana E, Risau W. Vascular endothelial growth factor induces VE-cadherin tyrosine phosphorylation in endothelial cells. J Cell Sci. 1998; 111:1853–65. [PubMed: 9625748]
77. Gavard J, Gutkind JS. VEGF controls endothelial-cell permeability by promoting the beta-arrestin-dependent endocytosis of VE-cadherin. Nat Cell Biol. 2006; 8:1223–34. [PubMed: 17060906]
78. Gampel A, Moss L, Jones MC, Brunton V, Norman JC, Mellor H. VEGF regulates the mobilization of VEGFR2/KDR from an intracellular endothelial storage compartment. Blood. 2006; 108:2624–31. [PubMed: 16638931]

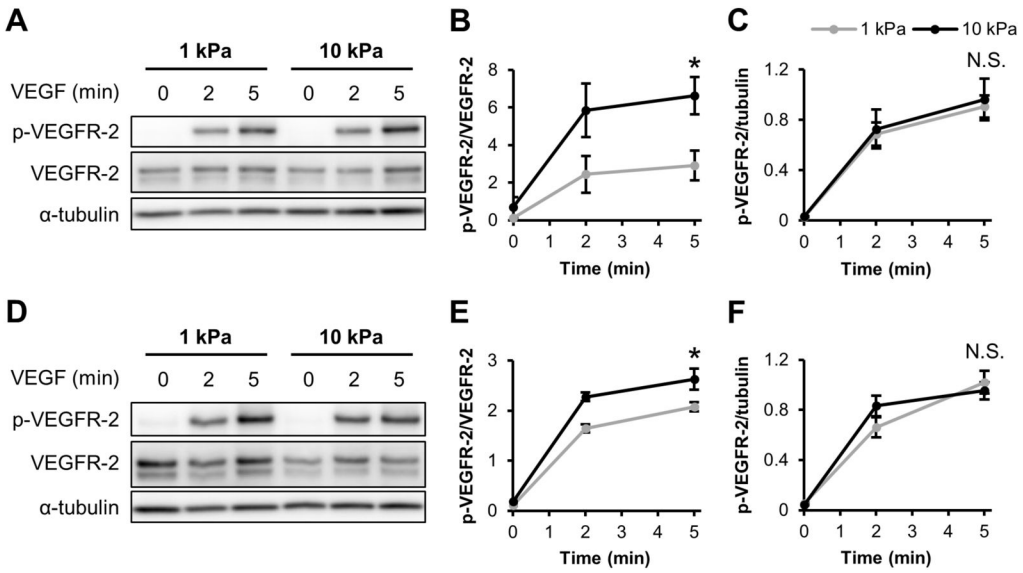

Figure 1.

Matrix stiffness enhances VEGF-induced VEGFR-2 response in endothelial cells independently of ECM protein type. (**A–C**) Sub-confluent HUVECs cultured on collagen-coated gels were stimulated with 5 ng/ml VEGF for the indicated amounts of time and probed for Y1175 VEGFR-2 phosphorylation and VEGFR-2 expression using a Western blot (**A**) with corresponding densitometry quantification (**B–C**). (**D–F**) Same as in (**A–C**) but HUVECs were cultured on fibronectin-coated substrates and analyzed for p-VEGFR-2 and VEGFR-2 using Western blot (**D**) and densitometry (**E–F**). α-tubulin was used as a loading control. Plots are mean ± SE. N = 3 independent sets of lysates. * $p<0.05$ from student's *t*-test. N.S. not significant.

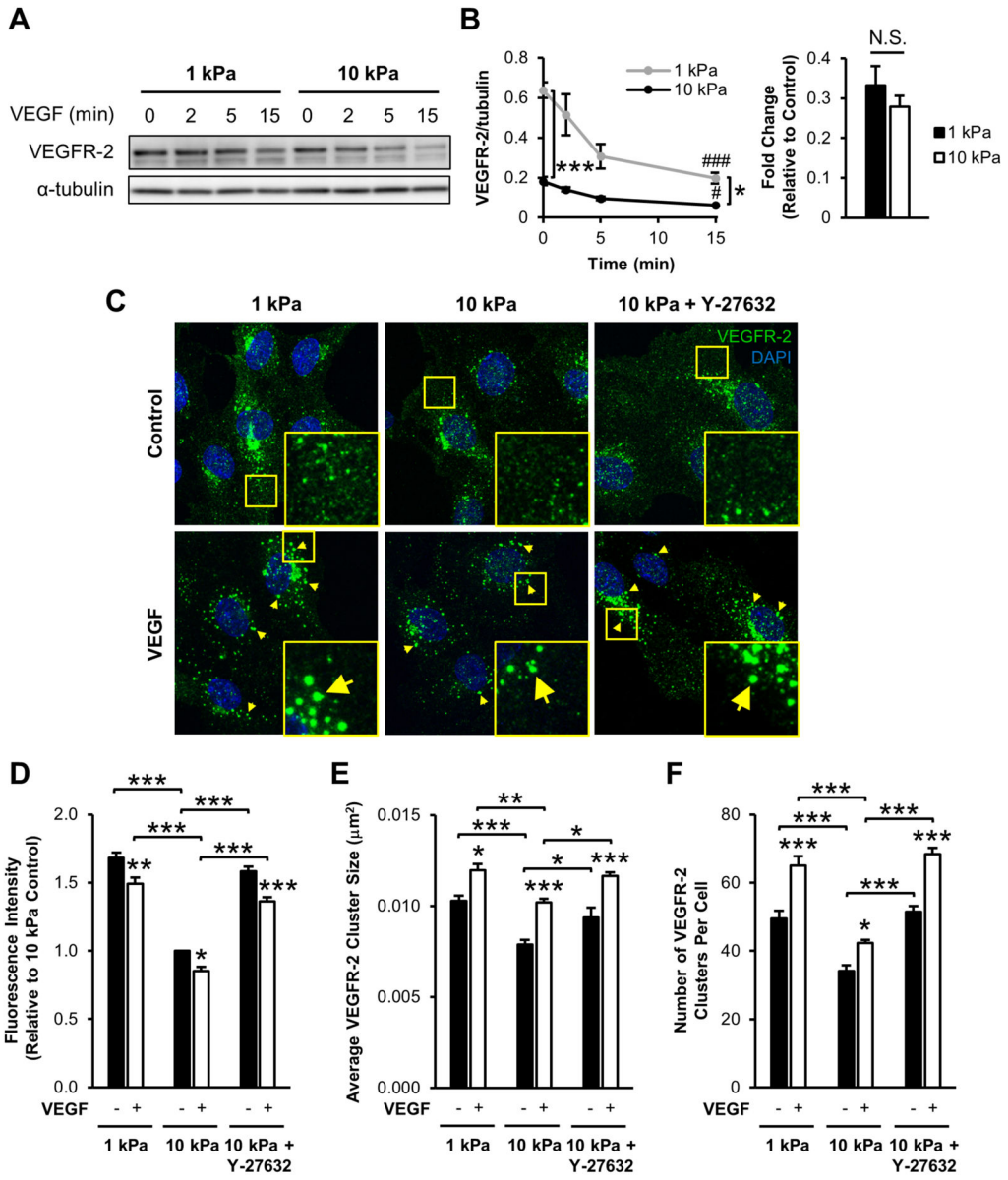

Figure 2.

VEGFR-2 expression level and clustering decreases with the addition of VEGF and as a function of ECM stiffness. (**A–B**) Sub-confluent HUVECs seeded atop collagen-coated gels were stimulated with 5 ng/ml VEGF for the indicated times and probed for VEGFR-2 expression by Western blot (**A**) and normalized VEGFR-2 densitometry (**B**). The fold change (VEGF/control) in densitometry quantification is also reported. α-tubulin was used as a loading control. Plots are mean ± SE. N = 3 independent sets of lysates. # $p<0.05$, ### $p<0.001$ compared to control sample at each stiffness. * $p<0.05$, *** $p<0.001$. (**C**) Sub-confluent endothelial cells cultured on collagen-coated 1 kPa, 10 kPa, or 10 kPa gels pretreated with 5 μM Y-27632 were cultured under control conditions (upper panel) or incubated with 5 ng/ml VEGF for 15 min (lower panel) and immunostained for VEGFR-2. Insert is a 3x zoom of the boxed region. Arrows indicate VEGFR-2 clusters formed after

VEGF treatment. Images were acquired with identical exposure settings (Scale bars, 20 μm). Quantification of normalized fluorescence intensity (**D**), average VEGFR-2 cluster size (**E**), and the average number of VEGFR-2 clusters per cell (**F**) for each condition. Plots are mean ± SE. N = 5 independent experiments, at least 30 cells per condition. * $p<0.05$, ** $p<0.01$, *** $p<0.001$ from ANOVA with post hoc Tukey's test. N.S. not significant.

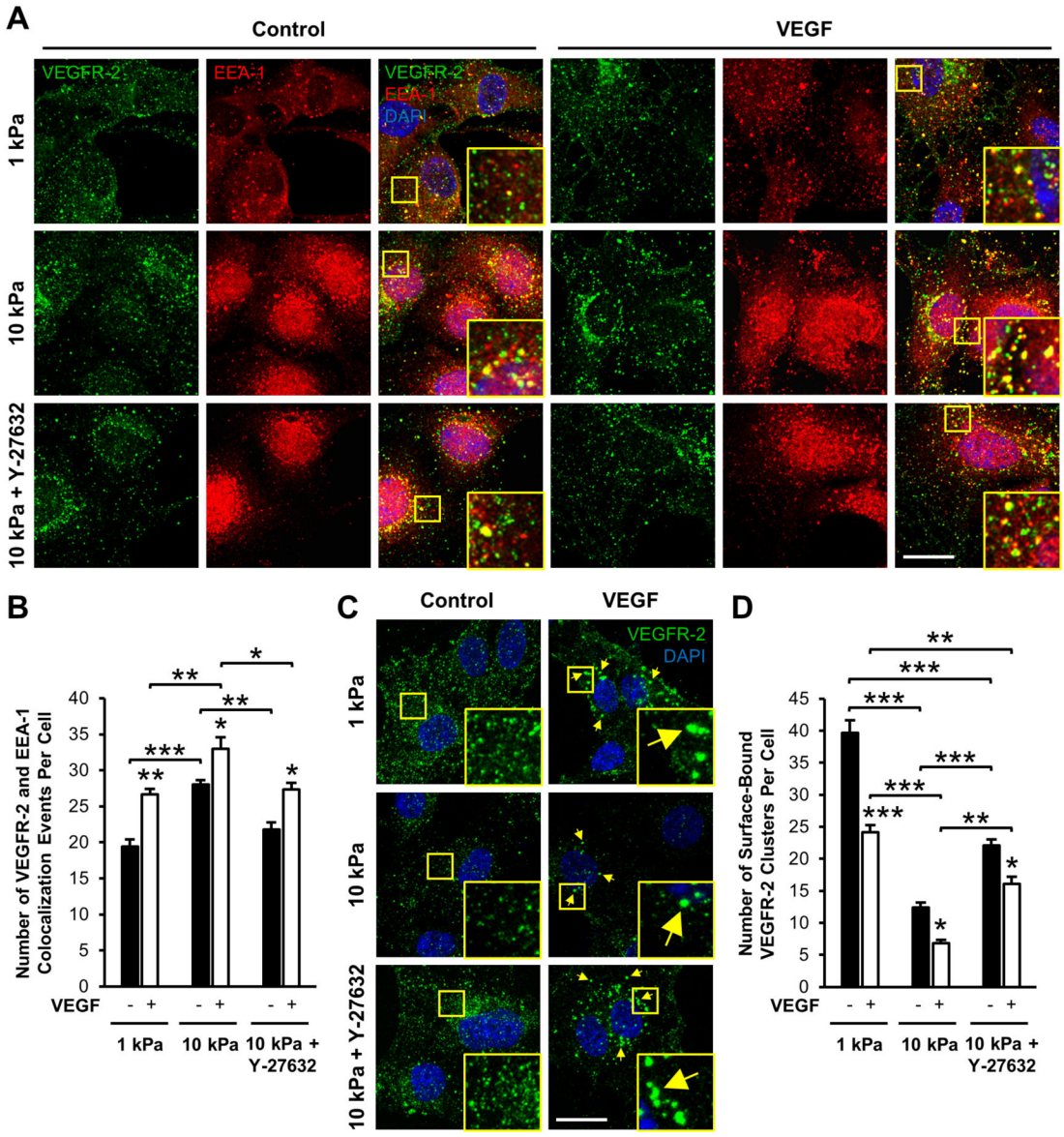

Figure 3.

Matrix stiffness and VEGF stimulation foster VEGFR-2 colocalization with EEA-1 and decrease cell surface VEGFR-2 levels in endothelial cells. (**A**) Sub-confluent HUVECs on 1 kPa, 10 kPa, or 10 kPa collagen-coated gels with Y-27632 pretreatment were cultured under control conditions (left panels) or stimulated with 15 min VEGF (right panels) and then co-stained for VEGFR-2 and EEA-1. Insert is a 3x zoom of the boxed region. Images were acquired with identical exposure settings (Scale bars, 20 μm). (**B**) The average number of VEGFR-2 and EEA-1 colocalization events per cell compared to control conditions. Plots are mean ± SE. N = 3 independent experiments, at least 30 cells per condition. (**C**) Non-permeabilized HUVECs were stained for VEGFR-2 following exposure to control conditions (left panel) or 15 min VEGF treatment (right panel) to visualize receptors located on the cell surface. Insert is a 3x zoom of the boxed region. Arrows indicate VEGFR-2 clusters formed after VEGF stimulation. Images were captured with identical exposure

settings (Scale bars, 20 μm). (**D**) Quantification of the average number of membrane-bound VEGFR-2 clusters per condition. Plots are mean ± SE. N = 3 independent experiments, at least 30 cells per condition. * $p<0.05$, ** $p<0.01$, *** $p<0.001$ from ANOVA with post hoc Tukey's test. N.S. not significant.

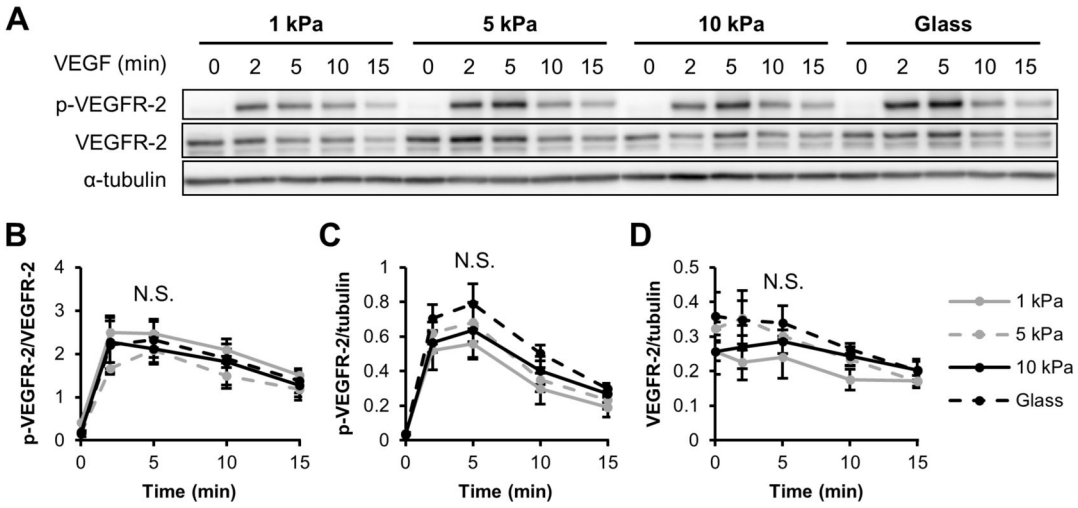

Figure 4.

Matrix stiffness does not influence VEGF-induced VEGFR-2 phosphorylation in confluent endothelial monolayers. (**A–D**) Confluent HUVECs on collagen-coated PA gels or glass were stimulated with 5 ng/ml VEGF for the indicated amounts of time, lysed, and analyzed for Y1175 p-VEGFR-2 and VEGFR-2 expression using a Western blot (**A**) and densitometry quantifications (**B–D**). α-tubulin was used as a loading control. Plots are mean ± SE. N = 3 independent sets of lysates. N.S. not significant.

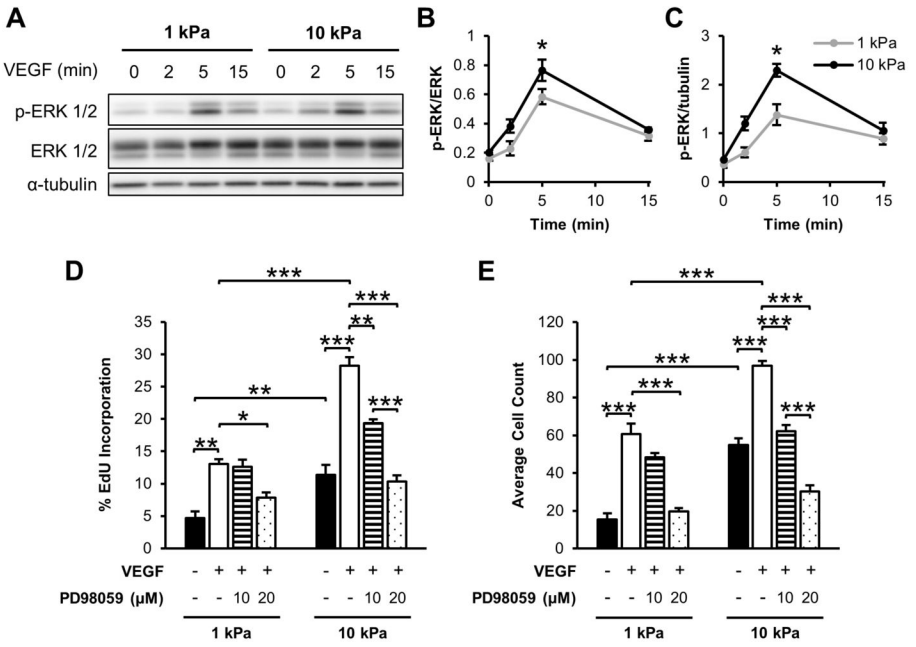

Figure 5.

Matrix mechanics regulate VEGF-mediated ERK 1/2 phosphorylation and proliferation in sub-confluent cells. (**A–C**) HUVECs cultured on collagen-coated gels were analyzed following 5 ng/ml VEGF treatment for T202/Y204 ERK 1/2 phosphorylation and ERK 1/2 expression through Western blot (**A**) and densitometry (**B–C**). α-tubulin was used as a loading control. Plots are mean ± SE. N = 3 independent sets of lysates. (**D**) Sub-confluent HUVEC proliferation after being stimulated with 5 ng/ml VEGF for 24 h with or without PD98059 pretreatment as determined by Click-iT EdU staining. Percentages relative to total cell number. N = 3 independent experiments, at least 300 cells per condition. (**E**) Average cell count from 15 representative fields of view. Plots are mean ± SE. N = 3 independent experiments. * $p<0.05$, ** $p<0.01$, *** $p<0.001$ from ANOVA with post hoc Tukey's test.

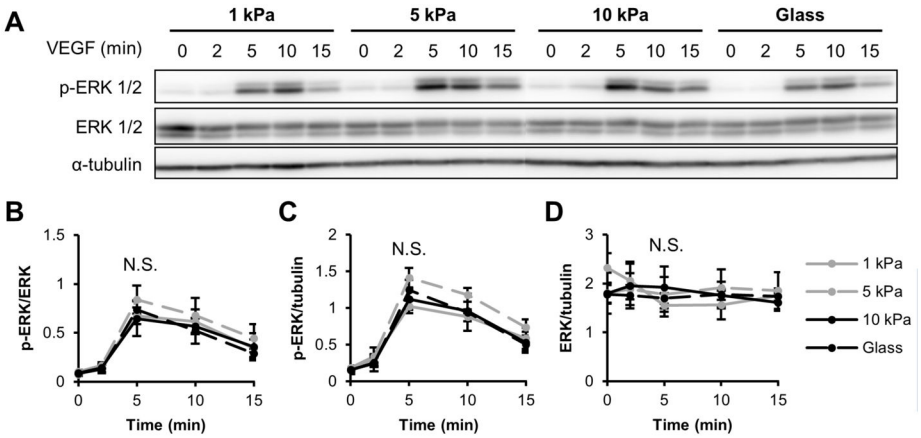

Figure 6.

VEGF-induced ERK 1/2 phosphorylation is not influenced by ECM compliance in confluent endothelial cells. (**A–D**) Following 5 ng/ml VEGF stimulation for the indicated amounts of time, confluent HUVECs on various stiffness collagen-coated gels or glass were probed for T202/Y204 ERK 1/2 phosphorylation and ERK 1/2 expression using a Western blot (**A**) and corresponding densitometry analysis (**B–D**). α-tubulin was used as a loading control. Plots are mean ± SE. N = 3 independent sets of lysates. N.S. not significant.

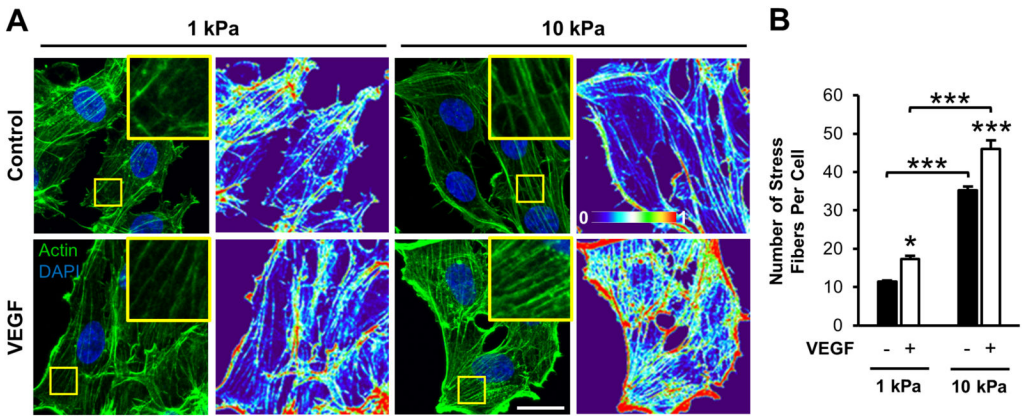

Figure 7.

Matrix stiffness and VEGF stimulate actin stress fiber formation in endothelial cells. (**A**) Phalloidin staining and corresponding fluorescence intensity heat maps of sub-confluent HUVECs on 1 or 10 kPa collagen-coated substrates under control conditions (upper panel) or 15 min VEGF stimulation (lower panel). Cells were counterstained with DAPI. Heat maps represent low (0) to high (1) intensity (A.U.). Insert is a 3x zoom of the boxed region. Images were acquired with identical exposure settings (Scale bars, 20 μm). (**B**) Quantification of the average number of stress fibers per cell for each condition. Plot is mean ± SE. N = 3 independent experiments, at least 30 cells per condition. * $p<0.05$, *** $p<0.001$ from ANOVA with post hoc Tukey's test.